The Journal of the Astronautical Sciences, Vol. 47, Nos. 3 and 4, July–December 1999, pp. 275–294

Modeling Issues Concerning Motion of the Saturnian Satellites

Steven G. Tragesser[1] and James M. Longuski[2]

Abstract

A study is performed to find the minimum-order model that can achieve an accuracy of 1 km in the dynamic propagation of the Saturnian satellites over a period of four years. The need for such an investigation has risen out of recent advances in the accuracy of orbit determination techniques that are to be used in the Cassini mission. Effects such as Saturn's rings, tides on Saturn and the satellites, gravity harmonics on Saturn and the satellites, other solar system bodies, small Saturnian satellites, coupling of the satellite attitudes with translational dynamics, and general relativity are considered. A conservative assessment of the effects that must be modeled is obtained with numerical simulation using a fixed set of initial conditions for the satellites. This simple method is shown to exaggerate the impact of new modeling effects, so a second method is employed where the initial conditions are adjusted in order to minimize the perturbations of new effects. The second method suggests that, in addition to the point mass interactions of the eight major Saturnian satellites, the minimum order model includes zonal harmonics of Saturn up through eighth order, Saturn's rings, Janus, the asphericities of Mimas and Enceladus, and the point mass effects of the Sun and Jupiter.

Introduction

Recent developments in navigation software and data acquisition have improved orbit determination to the point where modeling accuracy for a given planetary system is an issue that must be investigated. Since navigation is often based on the position relative to natural satellites, knowledge of the spacecraft state can be no better than that of the satellite ephemeris.

For the Cassini mission to Saturn, it is estimated that the dynamic model of the Saturnian satellites must be capable of achieving a 1 km accuracy in the satellite positions over a period of four years (corresponding to the duration of the mission) [1].

[1]Doctoral Candidate, School of Aeronautics and Astronautics, Purdue University, West Lafayette, IN 47907-1282. Currently, Assistant Professor, Department of Aeronautical and Astronautical Engineering, Air Force Institute of Technology, WPAFB, OH 45433-7765.
[2]Professor, School of Aeronautics and Astronautics, Purdue University, West Lafayette, IN 47907-1282. Member AAS. Associate Fellow AIAA.

This requirement is made so that the model does not limit the accuracy of the orbit determination.

In this paper, we find the minimum-order model that achieves the requirement for the eight major satellites of Saturn, which from nearest to farthest are Mimas, Enceladus, Tethys, Dione, Rhea, Titan, Hyperion and Iapetus. The method is primarily numerical so the results are specific to the Saturnian system, but the same techniques can be applied to other planetary systems. We investigate all gravity fields that may significantly affect the satellite positions, namely:

- Saturnian harmonics
- Sun and planets (point masses)
- Rings
- Saturnian tides (using Love numbers)
- Small satellites (Janus, Epimetheus, etc.)
- Harmonics and tides at the satellites
- Satellite attitude-translational coupling
- General relativity

Nongravitational forces (drag, collisions, radiation pressure, Lorentz force), oblateness of the Sun and exosolar system gravity fields (e.g. nearest star) are deemed to be insignificant and are not analyzed. Furthermore, the parameters associated with the gravity field (e.g. harmonic coefficients) are assumed to be known to sufficient accuracy such that uncertainty in these parameters is not a significant source of error (i.e. less than about 100 m over four years).

Modeling

The model of the Saturnian system is developed using a general form of the equations of motion that includes an inverse-square gravity field as the main term and an additional term representing all other gravitational influences. The acceleration on the ith body (of mass m_i) due to $n + 1$ mutually interacting particles (the planet and n satellites) and a perturbing acceleration, $\mathbf{A}_i$, is

$$\ddot{\mathbf{R}}^{OPi} = \sum_{\substack{j=1 \\ j\neq i}}^{n+1} \frac{Gm_j}{|\mathbf{R}^{OPj} - \mathbf{R}^{OPi}|^3}(\mathbf{R}^{OPj} - \mathbf{R}^{OPi}) + \mathbf{A}_i \tag{1}$$

where the time derivatives are with respect to an inertial frame, $\mathbf{R}^{OPi}$ is the position vector of the ith body with respect to a point fixed in that frame, and $i = 1, 2, \ldots, n + 1$. The first n position vectors refer to the satellites and the $(n + 1)$th position refers to the planet which will also be called $\mathbf{R}^{OS}$ for convenience. The perturbing acceleration, $\mathbf{A}_i$, accounts for such effects as the tides, rings, asphericity of the bodies, etc. Since $\mathbf{A}_i$ is often a function of coordinates that are relative to the planet, it is convenient to solve equation (1) in terms of position vectors with a reference point located at the planet, "S." Using the simple identity

$$\mathbf{R}^{OPi} = \mathbf{R}^{OS} + \mathbf{R}^{SPi} \tag{2}$$

in equation (1) yields

$$\ddot{\mathbf{R}}^{OS} + \ddot{\mathbf{R}}^{SPi} = \sum_{\substack{j=1 \\ j\neq i}}^{n} \frac{Gm_j}{|\mathbf{R}^{SPj} - \mathbf{R}^{SPi}|^3}(\mathbf{R}^{SPj} - \mathbf{R}^{SPi}) - \frac{Gm_S}{|\mathbf{R}^{SPi}|^3}\mathbf{R}^{SPi} + \mathbf{A}_i \tag{3}$$

where m_S is the mass of the planet. Setting $P_i = S$ in equation (3) we find

$$\ddot{\mathbf{R}}^{OS} = \sum_{j=1}^{n} \frac{Gm_j}{|\mathbf{R}^{SPj}|^3} \mathbf{R}^{SPj} + \mathbf{A}_S \tag{4}$$

Then substituting this expression into equation (3), we arrive at the final form of the equations of motion for relative coordinates

$$\ddot{\mathbf{R}}^{SPi} = \sum_{\substack{j=1 \\ j\neq i}}^{n} \frac{Gm_j}{|\mathbf{R}^{SPj} - \mathbf{R}^{SPi}|^3} (\mathbf{R}^{SPj} - \mathbf{R}^{SPi}) - \frac{Gm_S}{|\mathbf{R}^{SPi}|^3} \mathbf{R}^{SPi} + \mathbf{A}_i - \sum_{j=1}^{n} \frac{Gm_j}{|\mathbf{R}^{SPj}|^3} \mathbf{R}^{SPj} - \mathbf{A}_S \tag{5}$$

where $i = 1, 2, \ldots, n$. By solving for position relative to the planet, we have reduced the degrees of freedom from $3(n + 1)$ to $3n$. If we are interested in inertial positions or the motion of the planet, equation (4) must be reclaimed.

Equations (5) are integrated directly (by Cowell's method) using a Runge-Kutta-Verner fifth-order algorithm. We now investigate various perturbing accelerations.

Spherical Harmonics

The expansion for the gravity potential at coordinates r, λ, L (see Fig. 1) of an aspherical body of radius R_{pl} and mass M is [2]

$$U = -\frac{1}{r} GM \left\{ 1 - \sum_{l=2}^{\infty} \left(\frac{R_{pl}}{r} \right)^l J_l P_l(\sin L) + \sum_{l=2}^{\infty} \sum_{m=1}^{l} [C_{lm} \cos(m\lambda) + S_{lm} \sin(m\lambda)] P_{lm}(\sin L) \right\} \tag{6}$$

where J_l, C_{lm} and S_{lm} are coefficients determined by the asphericity of the body and P_{lm} are Legendre polynomials.

To find the acceleration on the ith satellite ($\mathbf{A}_i$ in equation (5)), the potential is differentiated with respect to the Cartesian coordinates. The acceleration on the planet, $\mathbf{A}_S$, is simply the reaction force per unit mass, found by summing the scaled $\mathbf{A}_i$'s from all the satellites.

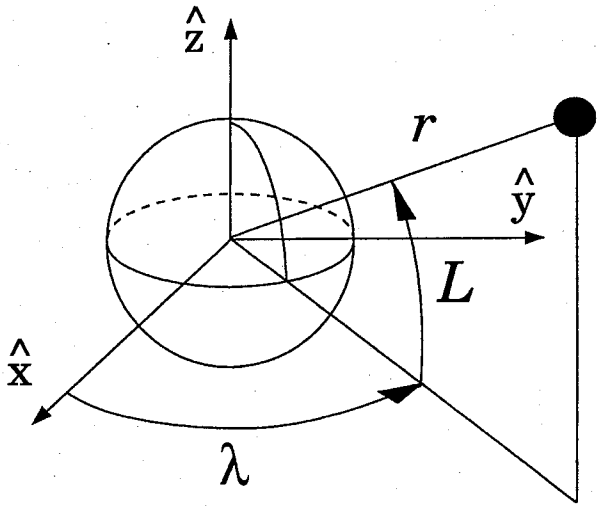

FIG. 1. Spherical Coordinate System.

Saturn Tides

The potential due to a tidal distortion in a body of mass m' located at (r', λ', L') is [3]

$$U = \sum_{l=2}^{\infty} \frac{Gm'k_l}{r'} \left(\frac{R_{pl}}{r'}\right)^l \left(\frac{R_{pl}}{r}\right)^{l+1} \left\{ P_l(\sin L) P_l(\sin L') + 2 \sum_{m=1}^{l} \frac{(l-m)!}{(l+m)!} \cos[m(\lambda - \lambda')] P_{lm}(\sin L) P_{lm}(\sin L') \right\} \tag{7}$$

where k_l are the dimensionless Love numbers [4]. Comparing equation (7) with equation (6), we see that the tides can be modeled as spherical harmonics with the time-varying coefficients:

$$J_l^* = -\left(\frac{m'}{M}\right) \left(\frac{R_{pl}}{r'}\right)^{l+1} k_l P_l(\sin L') \tag{8}$$

$$\left.\begin{matrix} C_{lm}^* \\ S_{lm}^* \end{matrix}\right\} = 2 \frac{(l-m)!}{(l+m)!} \left(\frac{m'}{M}\right) \left(\frac{R_{pl}}{r'}\right)^{l+1} k_l P_{lm}(\sin L') \times \begin{cases} \cos(m\lambda') \\ \sin(m\lambda') \end{cases} \tag{9}$$

We ignore orbital evolution due to energy dissipation from viscosity since it is only influential over much longer periods of time than we deal with in this study. Burns [5] and Peale *et al.* [6] include this effect in their analysis of tidal phenomena.

Rings

The accelerations at a point (x, y, z) due to a disk of radius a and density σ is [7]

$$\begin{aligned} \ddot{x} &= [-4G\sigma x a^{1/2}/(k\rho^{3/2})] \{(1 - \tfrac{1}{2}k^2)K(k) - E(k)\} \\ \ddot{y} &= [-4G\sigma y a^{1/2}/(k\rho^{3/2})] \{(1 - \tfrac{1}{2}k^2)K(k) - E(k)\} \\ \ddot{z} &= 2G\sigma(\rho^2 + z^2 + a^2 + 2\rho a)^{-1/2} K(k) - 2G\sigma \operatorname{sign}(z) \{\tfrac{\pi}{2} + \tfrac{\pi}{2} \operatorname{sign}(a - \rho) \\ &\quad - \operatorname{sign}(a - \rho) [(E(k) - K(k))F(\theta, k') + K(k)E(\theta, k')]\} \end{aligned} \tag{10}$$

where $K(k)$ and $E(k)$ are complete elliptic integrals of the 1st and 2nd kind, $F(\theta, k')$ and $E(\theta, k')$ are incomplete elliptic integrals of the 1st and 2nd kind and

$$\begin{aligned} \rho^2 &\equiv x^2 + y^2 \\ k^2 &\equiv 4\rho a/(\rho^2 + a^2 + 2\rho a) \\ k' &\equiv (1 - k^2)^{1/2} \\ \theta &\equiv \tan^{-1}|z/(\rho - a)| \end{aligned} \tag{11}$$

Similar formulations are in Scheeres and Vinh [8] and Lass and Blitzer [9]. To get the acceleration due to a disk with inner radius a_1 and outer radius a_2, we find the acceleration due to a disk of radius a_2 from equation (10) and subtract the acceleration due to a disk of radius a_1.

Satellite Attitude-Translational Coupling

The potential at a distance r from the center of mass of a satellite with mass m is [10]

$$U = -\frac{Gm}{r}\left[1 + \frac{1}{2mr^2}(I_x + I_y + I_z - 3I)\right] \tag{12}$$

where I_x, I_y, and I_z are the principal moments of inertia of the satellite and I is the moment of inertia about the line connecting the point of interest and the center of mass. This expression assumes that the largest dimension of the satellite is much smaller than the distance r.

Without loss of generality, we assume $I_x < I_y < I_z$. Then, to further simplify the analysis, we assume that the $\hat{\mathbf{x}}$ (longest) axis is always along the radial line to the planet and the $\hat{\mathbf{z}}$ (shortest) axis is normal to the orbit plane (so the body is synchronously locked in its stable configuration). The potential due to the satellite is then

$$U = -\frac{Gm}{r}\left[1 + \frac{1}{2mr^2}(-2I_x + I_y + I_z)\right] \tag{13}$$

Taking the derivative of the potential leads to the perturbing acceleration on the aspherical body with position $\mathbf{r}$ relative to the planet of mass M:

$$\mathbf{A}_i = \frac{3GM(2I_x - I_y - I_z)}{2m}\frac{\mathbf{r}}{r^5} \tag{14}$$

This force is aligned with the position vector because a principal axis of the satellite is always pointing toward Saturn.

Analysis could also be performed by modeling the satellite's aspherical gravity field using gravity harmonics. However, formulation (14) is more convenient for irregularly shaped satellites where a large number of harmonics may be required to obtain a reasonable approximation of the mass properties.

Other references in the literature include Goldreich and Peale [11] and Vinh [12] who deal with the special case of resonant spin rates and stability of satellite attitude dynamics.

Relativistic Effects

The perturbing acceleration provided by the parameterized post-Newtonian metric theory of gravitation is given by Mease *et al.* [13]:

$$\mathbf{A}_i = Gm\{[2(\beta + \gamma)(Gm/r) - \gamma(\dot{\mathbf{r}} \cdot \dot{\mathbf{r}})]\mathbf{r} + 2(1 + \gamma)(\mathbf{r} \cdot \dot{\mathbf{r}})\dot{\mathbf{r}}\}/(r^3c^2) \tag{15}$$

where c is the speed of light *in vacuo* and β and γ are the Eddington-Robertson-Schiff parameters. Nominal values of $\beta = \gamma = 1$ are used for the analysis here. This is equivalent to the formulation by Will [14], for a non-rotating reference frame.

Results for Fixed Initial Conditions

Baseline

To determine the effect of new additions to the dynamic model, a baseline reference must be constructed. Our baseline model is the model used in 1996

by the Navigation and Flight Mechanics Section at JPL. It consists of the following [1]:

- Mutual interactions of the eight major Saturian satellites (Mimas, Enceladus, Tethys, Dione, Rhea, Titan, Hyperion and Iapetus) modeled as point masses
- J2, J4 and J6 zonal harmonics of Saturn
- Gravitational perturbations due to the Sun and Jupiter

To verify our model, the positions of the satellites from our simulation of the baseline were compared to those of JPL (which we will henceforth refer to as the 1996 JPL baseline model). The differences in position over four years (1461 days) were less than 16 m.

The perturbation of a particular refinement to the dynamic model (e.g. addition of the ring gravity field) is defined to be the difference between the satellite positions from the baseline simulation and a simulation that includes the new effect. We first assume the initial conditions from the 1996 JPL model to be perfectly correct, so they are kept constant when introducing a new model. It turns out that this fixed initial condition approach exaggerates the perturbations, so small changes in the initial satellite states are considered in a later section.

Due to higher-order interactions, the changes in the dynamics of the system from a new modeling effect is dependent on the baseline model, so the results given below may vary somewhat for a different choice of baseline. For simplicity, we assume that new effects can be modeled as independent perturbations, so they can be addressed one at a time.

Higher-Order Zonals

We now investigate the effect of higher-order zonals (that is, terms of 8th order and higher) on the positions of the Saturnian satellites. First, we simulate the well-known effect of Saturn's oblateness (the J_2 term of equation (6)) to get a reference acceleration from which we can estimate the influence of higher-order terms. We numerically arrive at the effect due to oblateness by eliminating that term from the baseline model. The magnitude of the difference in the satellite position vectors, between the two simulations (the baseline and the one excluding J_2), Δr, is plotted in Fig. 2. The positions of the eight satellites change radically when oblateness is not included in the baseline; a maximum effect of 7.5×10^5 km is shown for Dione.

These perturbations are caused by precession of the argument of periapsis, ω, and the longitude of the ascending node, Ω. Since these precession rates are integral multiples of each other (for nearly circular, equatorial orbits) [2], the Δr will be periodic over long periods of time (see Fig. 2). However, for shorter lengths of time and for higher-order harmonics, the effect on position appears to be secular (as it does for the satellites with a large semi-major axis in Fig. 2). Thus, we can estimate the change in position for J_4 through J_{10} based on the apparent secular rate of change of Δr from the case of J_2.

Mimas is the most strongly influenced by the spherical harmonics (since it is closest to Saturn), so we will use its perturbation as the metric by which to assess how many terms must be accounted for in the zonals to achieve 1 km accuracy. The secular rate of change in the pertubation of Mimas' orbit, determined from the linear portion (the first 20 days) of Fig. 2 is

$$\frac{d}{dt}(\Delta r) = 6304 \text{ km/day} \tag{16}$$

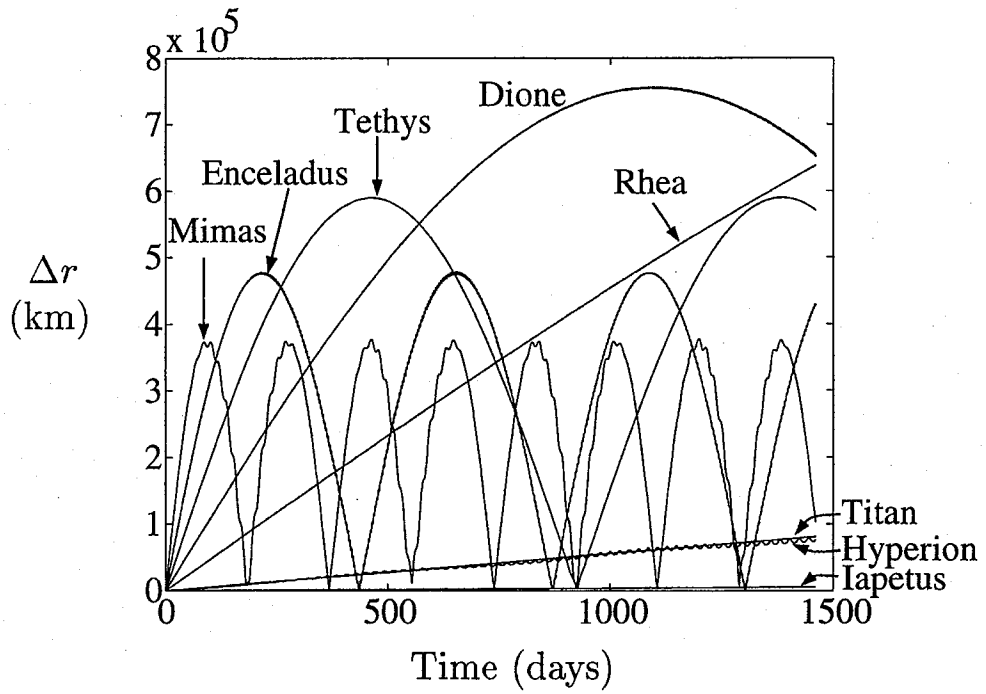

FIG. 2. Effect of J_2.

For nearly equatorial orbits, the lowest-order term ($1/r^{n+2}$ for J_n) dominates the accelerations derived from equation (6). From this term we can arrive at simple ratios between the J_2 acceleration and that of the higher-order harmonics. These are given in the second column of Table 1. Multiplying this ratio by the secular rate of change of Δr from equation (16) and a time of four years gives an approximation of the effect that a particular harmonic will have on Mimas. From Table 1 this estimate indicates that zonals must be included up through J_8 for 1 km accuracy.

The actual effects of the higher-order zonal harmonics are found numerically by including the appropriate force model, derived from equation (6), in the simulation. The plot for J_8 is shown in Fig. 3. The maximum effect matches the semi-analytic approximation quite closely. The secular change in position after four years is 10.9 km with a short period amplitude of 0.63 km. This indicates that this effect must be modeled for 1 km accuracy. The result for J_{10} (not shown) also matches the approximation very well. This term has a secular perturbation of 0.25 km with a short period amplitude of 0.04 km.

TABLE 1. Approximate and Actual Effects of the Zonal Harmonics on Mimas

n	J_n/J_2 Acceleration Ratio	Approximate Secular Effect (km)	Actual Secular Effect[a] (km)
4	7.38×10^{-3}	6.80×10^4	6.75×10^4
6	1.02×10^{-4}	940	950
8	1.17×10^{-6}	10.8	10.9
10	2.71×10^{-8}	0.25	0.25

[a]Found by numerical simulation.

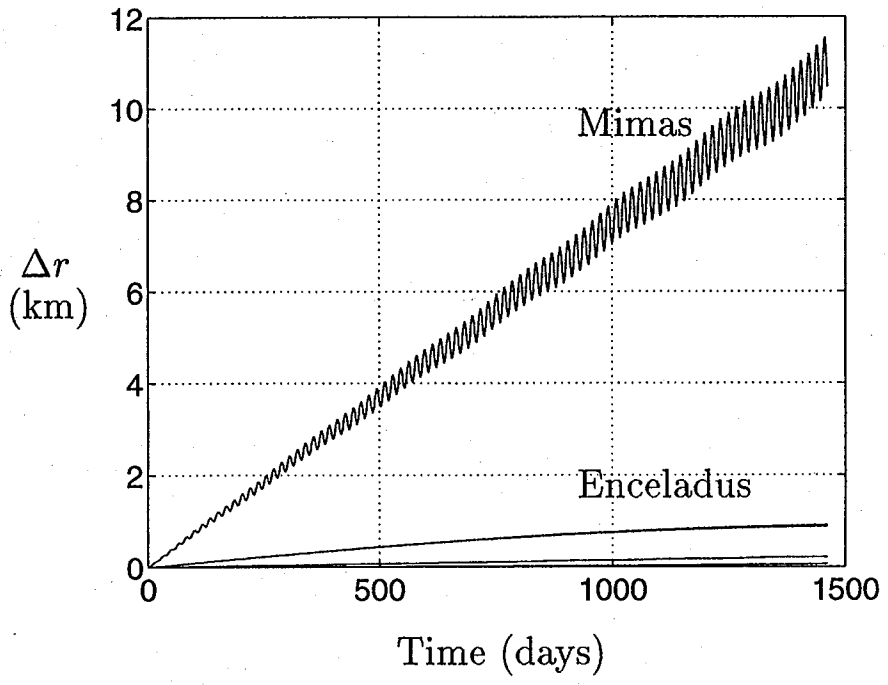

FIG. 3. Effect of J_8.

Tides

A tidal bulge forms on Saturn due to the gravitational pull of each of the satellites. Since Titan is the most massive satellite, we investigate the distortion due to this body first. Titan's mass and position are substituted into equation (9) to get the time-varying coefficients C_{22}^* and S_{22}^* which are then substituted into the potential function for an aspherical body (equation (6)).

The difference in the satellite positions between the baseline and the model including the tide caused by Titan is shown in Fig. 4. The perturbation to the orbit of Mimas is significant. After four years, the change in position is nearly 3 km and is primarily due to a secular change in true anomaly. (Tides caused by the gravitational pull of Dione, Tethys and Rhea are also investigated; maximum perturbations are given in Table 4. The tides due to Mimas, Enceladus, Hyperion, and Iapetus were approximated and found to be unimportant.)

This change in the true anomaly is due to a small change in the semi-major axis. There is no secular change in semi-major axis since the same amount of energy that is imparted to Mimas by the tidal bulge during one part of the orbit is taken away during the other part of the orbit. (See Burns [5] for a more complete description of the transfer of energy.) However, the mean value in the oscillation of a is not necessarily zero, depending upon the initial conditions.

To illustrate how bias occurs in the semi-major axis, we investigate a simple case of two bodies in coplanar, circular orbits. (See Figs. 5 through 7.) The tidal bulge on the planet is aligned with the outer, massive satellite. We simulate three sets of initial conditions to show the relationship between the initial geometry of the satellites and the bias in a of the small, inner satellite. If the bulge initially lags the inner satellite (Fig. 5), the transverse component of the gravity force is opposite

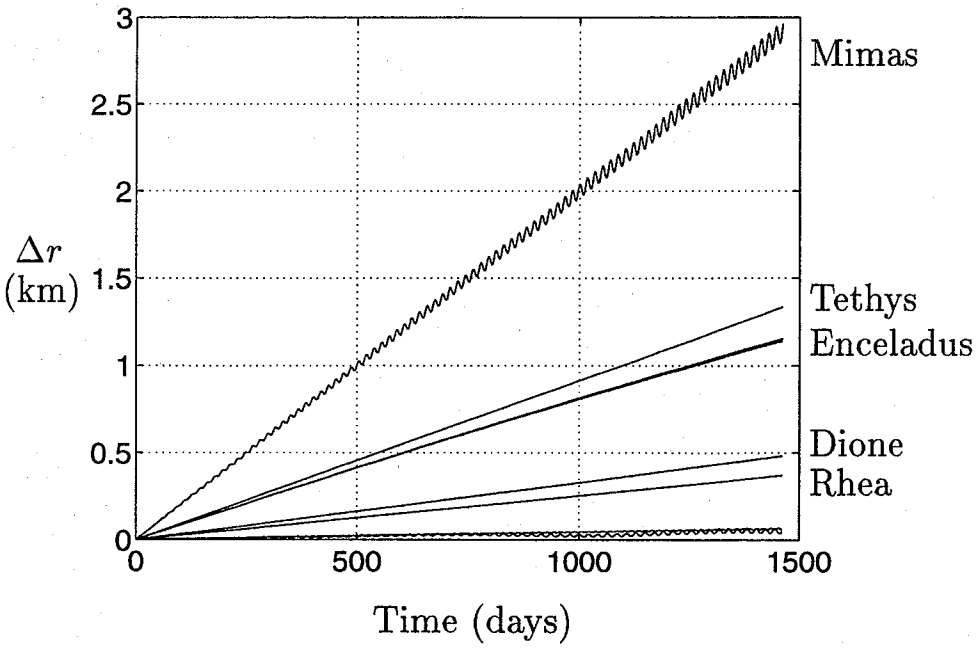

FIG. 4. Effect of the Saturn Tide Due to Titan.

the satellite velocity and a begins to decrease. The net amount of energy transferred to the inner satellite is zero over half of a synodic period ($\approx$0.29 days), so the semi-major axis returns to its initial size. However, the mean value of a has a negative bias and the period is therefore shorter than the baseline. Conversely, if the bulge initially leads the inner satellite (Fig. 6), the mass value of a is positive and the period is longer than the baseline. Halfway between these two cases there is no bias (Fig. 7) and the difference in position between the nominal and tidal simulations is minimized.

This case illustrates two faults in the simple approach of simulating the new modeling effect using the same 1996 JPL initial conditions that were used in the baseline (i.e. keeping fixed initial conditions between the two simulations). First, the size of the perturbation can be sensitive to the time at which the modeling effect is introduced. Second, a new modeling effect (that changes the gravity potential), in

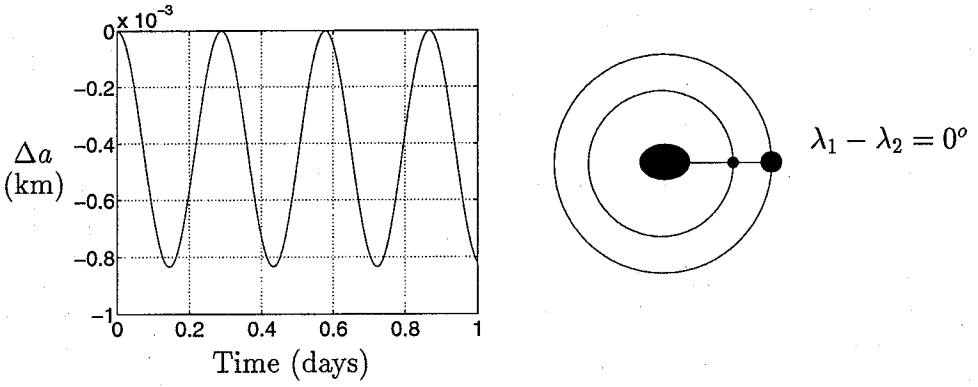

FIG. 5. Initial Orientation Causing a Phase Lag.

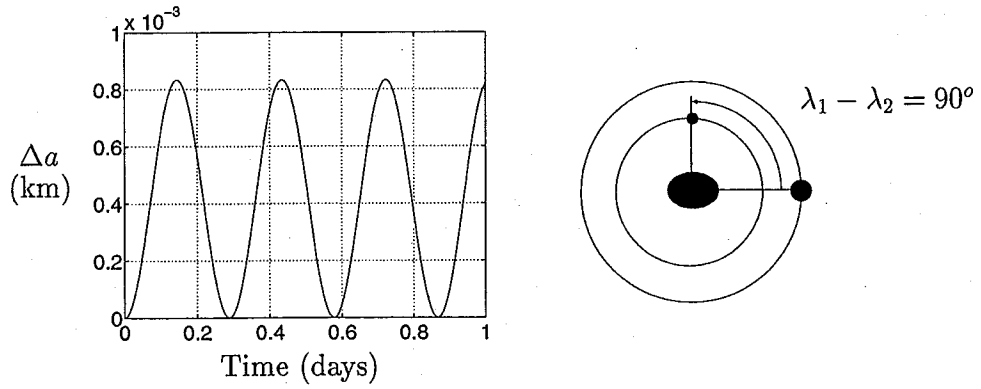

FIG. 6. Initial Orientation Causing a Phase Lead.

general, leads to a secular change in position because of the perturbation to the mean motion. This may exaggerate the actual effect since the mean motion is an invariant quantity that is known *a priori* (e.g. Titan has been observed for over 300 years and its period is well known). Both of these problems can be minimized or eliminated by an appropriate change in the initial conditions when simulating the new modeling effect. This is addressed later in the paper.

Satellite Attitude-Translational Coupling

Distortions away from sphericity have not been directly observed for the Saturnian satellites, so we must rely on theoretical values to determine the inertia properties. Zharkov *et al.* [15] provide values for the semiaxes of the satellites by assuming equilibrium of the tidal and centrifugal potential. Conservative values (based on uniform satellites) for the semiaxes a (directed at the planet), b (along the orbital motion) and c (perpendicular to the orbital plane) are given in Table 2. Except for the irregular satellite Hyperion, the largest deviations from the mean radius occur at Mimas where the tidal force and spin rate are largest.

From a, b and c we obtain the inertia properties for an ellipsoid which we then use in equation (14) to simulate the effect of asphericity. The perturbation of the position of Mimas reaches a maximum of 390 km in 4 years which is almost entirely due to a secular change in true anomaly. Effects for Enceladus, Tethys, Dione, Rhea

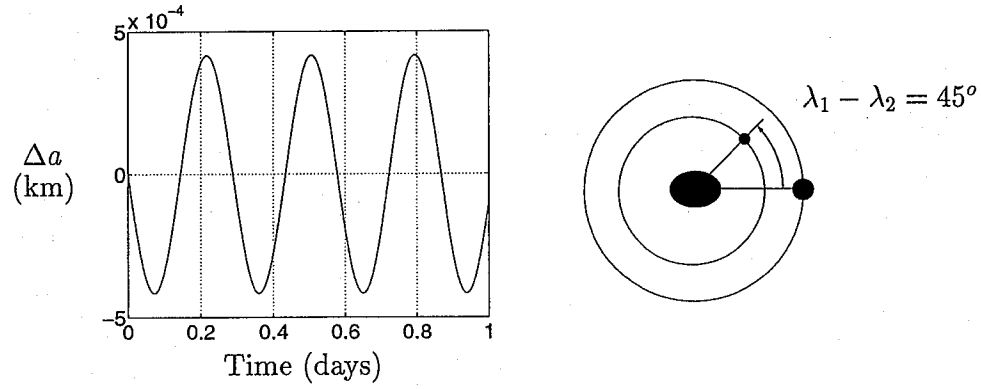

FIG. 7. Initial Orientation Causing No Phase Change.

TABLE 2. Semiaxes of Saturn's Satellites [15][a]

Satellite	a (km)	b (km)	c (km)
Mimas	214.5	201.4	197.0
Enceladus	259.8	252.5	250.0
Tethys	541.6	532.9	530.0
Dione	570.0	561.2	560.0
Rhea	767.7	765.7	765.0
Titan	2575.5	2575.1	2575.0
Hyperion	175.0	120.0	100.0

[a]No values are provided for Iapetus.

and Titan (see Table 4) are also significant. While Hyperion seems a likely candidate for investigation because of its irregular shape, it tumbles chaotically. Thus, the effect of Hyperion's asphericity should average out, so we will not consider it here.

Other Solar System Bodies

There are several bodies external to the Saturnian system that must be investigated. The results from a simple force analysis are presented in Table 3 to indicate the worst-case effects due to other bodies at their closest approach distances. The criterion is that the relative acceleration must be less than 1×10^{-15} km/s^2 for a change in Iapetus's position of less than 1 km in 4 years. These results are only a rough approximation and are overly conservative. However, they can be used to rank order the relative effects of the planets.

From the simple force analysis, Jupiter should have the largest effect. Simulation shows that a maximum perturbation of 250 km occurs at Iapetus. Uranus is the next candidate from Table 3. The effect due to this planet (also found by simulation) of 680 m is less than the 1 km requirement. The list in Table 3 indicates that all the other planets will have a smaller effect, so Jupiter is the only planet that must be included for 1 km modeling accuracy.

Rings

Equations (10) are propagated for a ring mass of 3×10^{-7} Saturn masses, which is the upper bound assumed by Campbell and Anderson [16]. Uniform density is assumed with an inner radius of 70,000 km (corresponding to the C Ring) and an

TABLE 3. Accelerations Due to Other Solar System Bodies

Planet	Perturbation acceleration (km/s^2)
Mercury	2.5×10^{-16}
Venus	4.3×10^{-15}
Earth	5.8×10^{-15}
Mars	7.5×10^{-16}
Jupiter	1.4×10^{-11}
Uranus	5.8×10^{-14}
Neptune	7.1×10^{-15}
Pluto	1.1×10^{-18}

outer radius of 137,000 km (corresponding to the A Ring) [5]. The results are given in Fig. 8 and show that the rings have a large impact on the satellite motion.

To investigate how the rings affect the satellites, the perturbations (between the baseline and ring simulations) to true anomaly, $\Delta\theta$, argument of periapsis, $\Delta\omega$, and longitude of ascending node, $\Delta\Omega$, are plotted in Fig. 9. (Changes in the elements a, e and i are not plotted because they are nearly constant.) The mechanics involved here are very similar to those of J_2. The gravitational attraction of the ring causes a secular change in Ω and ω and the ratio between the slopes of these two variables, 1/2, is the same as for the case of oblateness.

A smaller estimate for ring mass [16], 3×10^{-8} Saturn masses, is also investigated. The maximum effect (at Mimas) of 150 km shows that decreasing the ring mass by an order of magnitude decreases the effect linearly.

Summary and Simultaneous Simulation of All Effects

A compilation of the results from the previous subsections is given in Table 4. The maximum perturbation of each satellite is given for all the effects considered that are not already contained in the 1996 JPL baseline model. Effects which decrease the mean motion (or yield a negative slope for the equatorial phase angle) are given a negative sign by convention, since the perturbation in position tends to cancel effects that increase the mean motion. These perturbations are so large that we only provide 1 km resolution. As described above (in the section on tides), the errors produced by using fixed initial conditions from the 1996 JPL baseline exaggerate the influence of the new effects. A method for reducing this artificial amplification is discussed in the section entitled "Results for Adjusted Initial Conditions."

We investigate the validity of the assumption that new modeling effects are independent by *simultaneously* propagating all the effects. The maximum difference between the baseline and the dynamic model including all of the perturbations is given

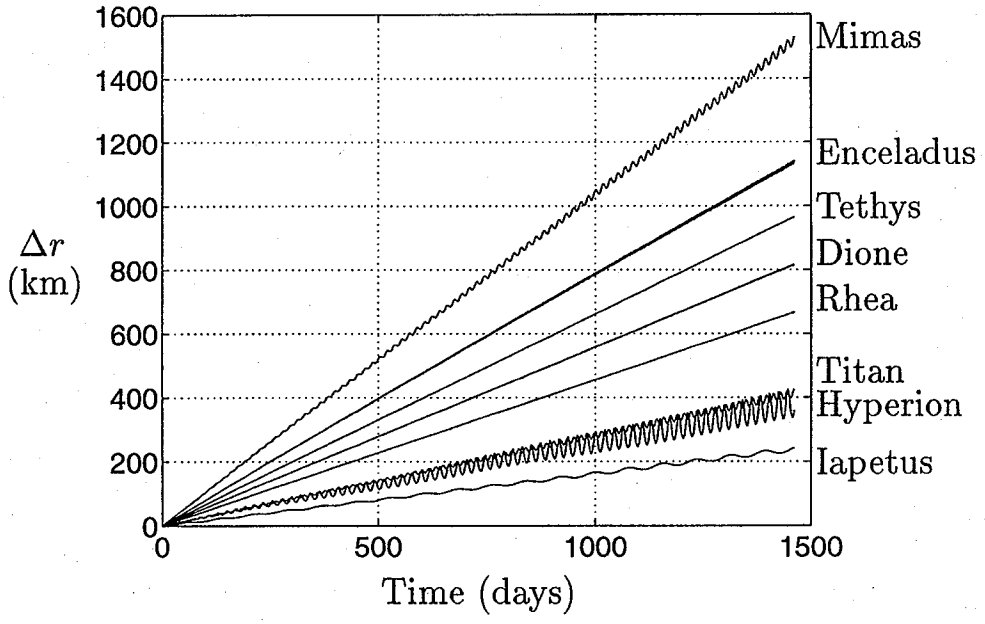

FIG. 8. Effect of Saturn's Rings (Annulus Model).

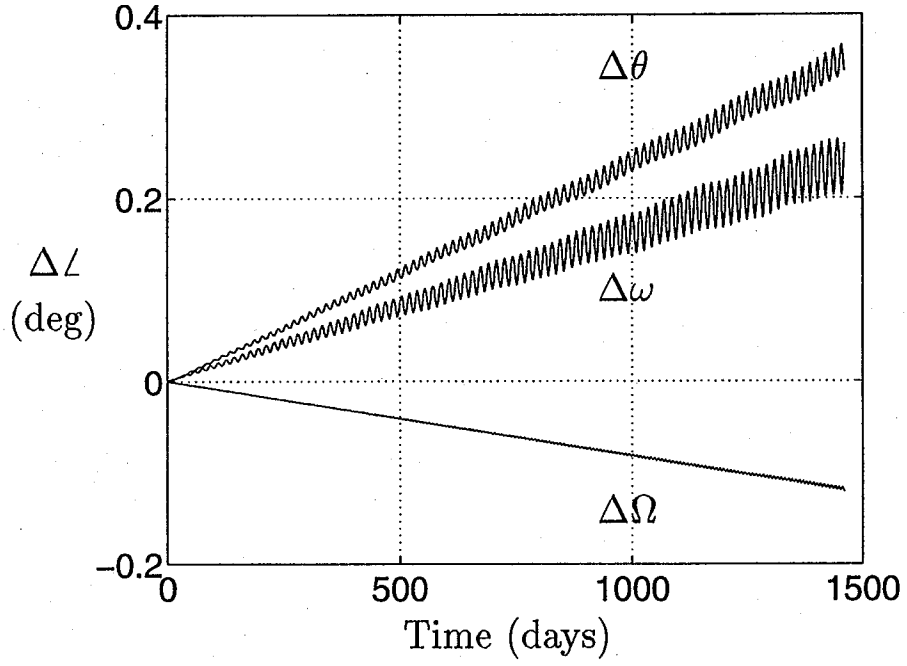

FIG. 9. Ring Effect on Orbital Elements of Mimas (Fixed IC's).

in Table 4 under "Simulation Result." The maximum perturbation at Mimas is 2033 km after 4 years. This closely matches the value of 2032 km determined by arithmetic addition of the individual perturbations to Mimas given in Table 4. Similar agreement occurs at all the satellites when comparing the simulation to the addition of individual perturbations, indicating that a superposition rule holds for variations in the gravity model.

These results imply that the only effects in Table 4 that do not have to be modeled (for 1 km accuracy) are the asphericity of Titan, J_{10}, Uranus, and the Saturn tide due to Rhea. This provides a very conservative bound for the phenomena that must be modeled.

Equivalence of Rings and Spherical Harmonics

The similarities in the behavior caused by oblateness and the rings raises the question of whether the rings can be modeled using gravity harmonics. The potential of a thin disk of uniform density σ and radius a is

$$U = -G\sigma\int_0^a\int_0^{2\pi}\frac{x\,d\phi\,dx}{\sqrt{x^2 + r^2 - 2xr\cos L\cos\phi}} \tag{17}$$

where r and L are the spherical coordinates of the point of interest (assumed here to be outside of the rings) as shown in Fig. 1 and x and ϕ are the polar coordinates of a differential element of the disk. Using a series expansion, it is straightforward to obtain the expression

$$\sqrt{x^2 + r^2 - 2xr\cos L\cos\phi} = \frac{1}{r}\sum_{n=0}^{\infty}\left(\frac{x}{r}\right)^n P_n(\cos L\cos\phi) \tag{18}$$

TABLE 4. Summary of Effects (Fixed IC's)[a]

Effect	Satellite							
	Mimas	Enc.	Tethys	Dione	Rhea	Titan	Hyper.	Iapetus
Rings	1529	1141	965	816	665	423	423	242
Mimas Asphericity	390	0	0	0	0	0	0	0
Enceladus Asphericity	0	126	0	2	0	0	0	0
Tethys Asphericity	3	0	216	0	0	0	0	0
Dione Asphericity	0	17	0	112	0	0	0	0
Rhea Asphericity	0	0	0	0	17	0	0	0
Titan Asphericity	0	0	0	0	0	1	1	0
Janus	110	34	4	30	1	−14	−14	−8
Epimetheus	10	−8	6	−3	4	7	6	3
General Relativity	−25	−18	−12	−8	−5	−1	−1	0
J_8 of Saturn	12	1	0	0	0	0	0	0
J_{10} of Saturn	0	0	0	0	0	0	0	0
Tethys Tide	5	1	0	0	0	0	0	0
Dione Tide	0	4	1	0	0	0	0	0
Titan Tide	−3	−1	−1	0	0	0	0	0
Rhea Tide	1	0	0	0	0	0	0	0
Uranus	0	0	0	0	0	0	0	1
Total Sum	2032	1297	1179	949	682	416	415	238
Simulation Result	2033	1296	1179	948	681	416	418	238

[a]Perturbations with respect to the 1996 JPL baseline model to 1 km accuracy.

Substituting equation (18) into equation (17) and integrating gives the following potential for the disk

$$U = -\frac{GM_{disk}}{r}\left[1 - \frac{1}{4}\left(\frac{a}{r}\right)^2 P_2(\sin L) + \frac{1}{4}\cdot\frac{3}{6}\left(\frac{a}{r}\right)^4 P_4(\sin L)\right.$$

$$\left. - \frac{1}{4}\cdot\frac{3}{6}\cdot\frac{5}{8}\left(\frac{a}{r}\right)^6 P_6(\sin L) + \cdots\right] \tag{19}$$

which agrees with Danby [17]. This is the same form as the potential of an aspherical body, given by

$$U = -\frac{GM_{pl}}{r}\left[1 - J_2\left(\frac{R_{pl}}{r}\right)^2 P_2(\sin L) - J_4\left(\frac{R_{pl}}{r}\right)^4 P_4(\sin L)\right.$$

$$\left. - J_6\left(\frac{R_{pl}}{r}\right)^6 P_6(\sin L) + \cdots\right] \tag{20}$$

Thus, the system of Saturn and its rings is equivalent to a single aspherical body with the following characteristics:

$$
\begin{aligned}
GM_{eq} &= GM_{pl} + GM_{disk} \\
(J_2)_{eq} &= J_2 \frac{GM_{pl}}{GM_{eq}} + \frac{1}{2} \frac{GM_{disk}}{GM_{eq}} \left(\frac{a}{R_{pl}} \right)^2 \\
(J_4)_{eq} &= J_4 \frac{GM_{pl}}{GM_{eq}} + \frac{1}{2} \cdot \frac{3}{6} \frac{GM_{disk}}{GM_{eq}} \left(\frac{a}{R_{pl}} \right)^4 \\
(J_6)_{eq} &= J_6 \frac{GM_{pl}}{GM_{eq}} + \frac{1}{2} \cdot \frac{3}{6} \cdot \frac{5}{8} \frac{GM_{disk}}{GM_{eq}} \left(\frac{a}{R_{pl}} \right)^6
\end{aligned}
\tag{21}
$$

From equation (21) we find that the effect due to the rings is indistinguishable from the zonal harmonics if Saturn's mass and zonal harmonics are unknown. In this case, the ring mass cannot be determined from the satellite dynamics. On the other hand, if Saturn's mass or zonal harmonics can be accurately calculated by some means other than the satellite dynamics (e.g. hydrostatic equilibrium calculations), then the satellite dynamics can be used to calculate ring mass.

The values of the equivalent zonal coefficients (for a ring mass of 3×10^{-7} Saturn masses) are given in Table 5. When comparing the two ring models (elliptic functions versus a series of zonal harmonics), terms up through the J_{16} zonal harmonic must be modeled in order to achieve 1 km accuracy over 4 years (for fixed initial conditions). When compared to the zonal coefficients of Saturn [3, 16], we see that the equivalent harmonic coefficients, calculated from equations (21), are much larger for order J_8 and higher. (In the absence of any data in the literature, zonals higher than J_{10} are set to zero for Saturn.) This suggests that the ring mass is the primary contributor to the higher-order zonal coefficients that would be observed from the satellite dynamics.

Results for Adjusted Initial Conditions

Method

We have seen how keeping the 1996 JPL baseline initial conditions (IC's) fixed when adding a new modeling effect can exaggerate the difference between the new model and the baseline by perturbing the mean motion of the satellites. To minimize this problem we can keep the mean motion invariant with an adjustment to the IC's since the period of an orbit is sensitive to changes in position and velocity.

We can reduce the difference between the baseline and the new modeling effect even further by changing the mean motion so that the phase angle in Saturn's

TABLE 5. Saturn Zonal Harmonics and Equivalent Harmonics for Ring System

Parameter	Value attributed to Saturn [3, 16]	Equivalent value of ring/planet system
J_2	1.62980×10^{-2}	1.629848×10^{-2}
J_4	-9.150×10^{-4}	-9.163×10^{-4}
J_6	1.030×10^{-4}	1.073×10^{-4}
J_8	-1.0×10^{-5}	-2.6×10^{-5}
J_{10}	2.0×10^{-6}	6.3×10^{-5}
J_{12}	0	-2.5×10^{-4}
J_{14}	0	1.0×10^{-3}
J_{16}	0	-4.4×10^{-3}

equatorial plane is matched between simulation of the baseline and the new model. Most of the satellites are in nearly circular, equatorial orbits, so precession of the longitude of the ascending node and precession of the argument of periapsis are dynamically similar to changes in the mean motion of the satellite. (Of course, as the orbit becomes more circular and more equatorial these angles become indistinguishable.) Therefore, we can approximately match the equatorial plane phase angle by removing any secular effects in $\Delta\Omega + \Delta\omega + \Delta\theta$. Precession of the node and line of apsides is insensitive to small changes in the satellite states, so a zero mean for $\Delta\Omega + \Delta\omega + \Delta\theta$ is attained primarily by manipulating the mean motion.

Illustrative Example

We will now demonstrate our method of adjusting IC's for the analysis of Saturn's rings. Since maintaining a zero mean for the in-plane phase angle involves only one degree of freedom, we elect to keep the initial osculating elements e_0, i_0, Ω_0, ω_0, and θ_0 invariant. Following this procedure, we calculate the desired adjustment to the initial position and velocity of Mimas (with respect to the 1996 JPL IC's) to be

$$\begin{aligned} \Delta\mathbf{r}_0 &= (-33\hat{\mathbf{x}} - 26\hat{\mathbf{y}} + 5\hat{\mathbf{z}})\ \text{m} \\ \Delta\mathbf{v}_0 &= (0.43\hat{\mathbf{x}} - 0.61\hat{\mathbf{y}} - 0.01\hat{\mathbf{z}})\ \text{mm/sec} \end{aligned} \tag{22}$$

Propagating the ring model for this altered set of IC's yields a maximum perturbation of 20 km after 4 years. This is only 1.3% of the effect for fixed IC's shown in Fig. 8 (which is 1530 km for Mimas). The change in the initial state is vanishingly small compared to the known accuracy of these variables.

The perturbations of the true anomaly, argument of periapsis, and longitude of the node are plotted in Fig. 10. When comparing this plot to Fig. 9, we see that adjustment of the IC's has not changed the slopes of $\Delta\omega$ and $\Delta\Omega$ (although the short period amplitude appears somewhat diminished). With the adjustment in equation (22), however, we are able to cause a slower mean motion that offsets the precession of the node and line of apsides.

Results

The IC's were adjusted to match the equatorial plane phase angle for all of the modeling effects considered above. The maximum perturbation of each satellite (to 0.01 km resolution) is given in Table 6 for each effect considered. In most cases, the perturbations for fixed IC's are reduced by more than an order of magnitude. We assign negative values to effects that precess the line of apsides opposite the direction of mean motion and to effects that precess the line of nodes in the $+\hat{\mathbf{z}}$ direction. These tend to offset the perturbation of the positive effects.

In our approach we assume that perturbations to each of the satellites are independent (individual changes in the IC's do not account for satellite interaction). Therefore, in cases of resonance, where coupling between satellites is significant, our method is not as effective in reducing the maximum perturbation. The most obvious example is the Saturn tide caused by Dione. Due to the 2:1 resonance between Dione and Enceladus, the perturbation of 3.9 km occurring at Enceladus for fixed IC's is only reduced to 0.85 km for adjusted IC's (see Table 6).

In some cases the resonance could be somewhat compensated for by special consideration of the IC adjustment. To illustrate the method, we take the case of adding Janus to the baseline model. For fixed IC's, Janus perturbs the positions of both

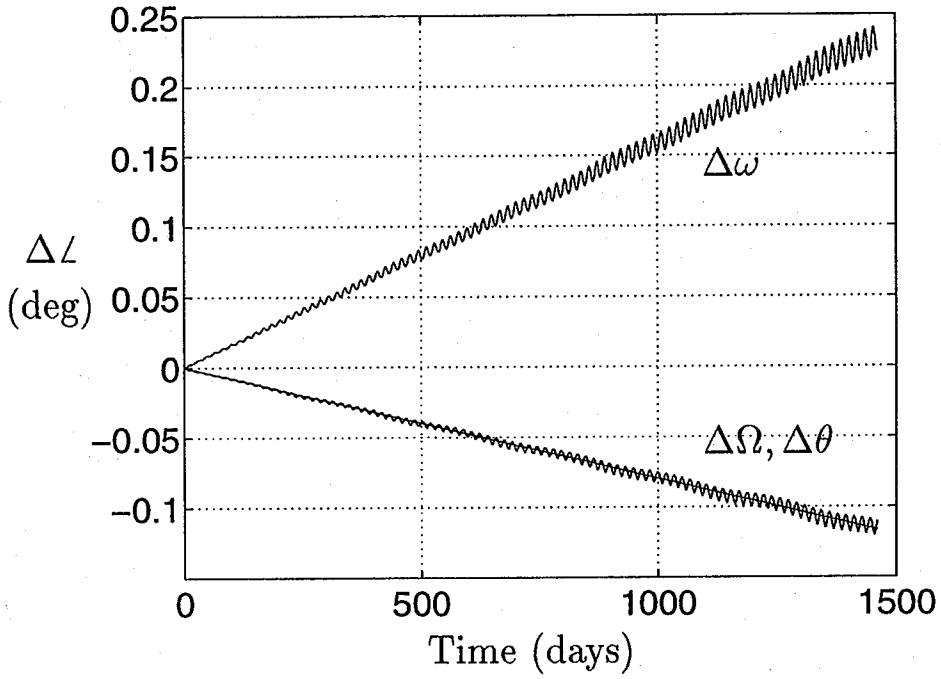

FIG. 10. Ring Effect on Orbital Elements of Mimas (Adjusted IC's).

Titan and Hyperion by 14 km (as shown in Table 4). Using this perturbation to determine new IC's for Hyperion leads to poor results since most of the 14 km effect occurs indirectly through the 4:3 resonance with Titan. To eliminate this interdependence of the satellite perturbations, we perform new simulations (of both the

TABLE 6. Summary of Effects (Adjusted IC's)[a]

Effect	Satellite							
	Mimas	Enc.	Tethys	Dione	Rhea	Titan	Hyper.	Iapetus
Rings	19.5	4.6	1.2	0.30	0.09	0.16	0.80	0.37
Mimas Asphericity	8.2	0	0.07	0	0	0	0	0
Enceladus Aspher.	0	4.0	0	0.75	0	0	0	0
Janus	1.8	0.60	0.12	0.02	0.01	0.03	−0.15	0.24
J_8 of Saturn	1.1	0.33	0.01	0.03	0.01	0.02	0.04	0.08
Tethys Asphericity	0.07	0	−0.05	0	0	0	0	0
Dione Asphericity	0	−0.21	0	0.29	0	0	0	0
Rhea Asphericity	0	0	0	0	0.03	0	0	0
Titan Asphericity	0	0	0	0	0	0.04	0.09	0
Epimetheus	0.35	0.48	0.02	0.05	0.01	0.03	0.07	0.09
General Relativity	0.56	0.82	0.04	0.09	0.01	0.05	0.24	0
Tethys Tide	0.14	0.08	0.15	0.02	0	0	0.05	0
Dione Tide	0.01	−0.85	0	0.11	0	0	0	0
Titan Tide	0	0.01	0	0	0	0.01	−0.02	0
Rhea Tide	−0.01	0.01	0	0.01	0.02	0.01	0.05	0
Total Sum	31.7	9.87	1.56	1.67	0.18	0.35	1.17	0.78
Simulation Result	29.1	7.76	1.18	1.02	0.38	0.73	5.07	2.16

[a]Perturbations with respect to the 1996 JPL baseline model to 0.01 km accuracy.

baseline and the baseline plus Janus) *without* Titan in order to isolate the direct effect of Janus on Hyperion and to determine the necessary differential correction to the 1996 JPL IC's. (The analogous simulation without Hyperion is not required since Hyperion is so small that its influence on Titan is negligible.) Using this approach, the maximum perturbation at Hyperion is only 0.15 km (in the simulation with Titan reinstated) as opposed to 4.0 km for the unmodified method.

Deducing the Minimum-Order Model

To determine whether the superposition rule observed for fixed IC's applies when secular changes in phase angle have been removed, we adjust the IC's for a simulation including all the effects from Table 6. The difference between the baseline and this all-inclusive simulation is given under "Simulation Result" in Table 6. The maximum change in the position of Mimas is reduced to 29 km for adjusted IC's (versus 2033 km for fixed IC's). Adding the perturbations from the right column of Table 6 yields a value of 32 km, so arithmetic addition of individual effects appears to apply. The rule is least accurate when coupling is significant in the satellite dynamics as in the case of Hyperion (due to resonance with Titan).

We now deduce the minimum-order model that achieves a 1 km accuracy, where the simultaneous simulation of all effects is taken to be the truth model. To arrive at the minimum model, we eliminate unimportant effects from the truth model and estimate the resulting perturbation to each satellite. Using the data in Table 6 and the rule of arithmetic addition, we find that the last ten items in Table 6 do not need to be modeled for 1 km accuracy. By adding the individual perturbations from these terms, an error of 1.1 km is predicted for Mimas when this model is compared to the truth model. Thus, the minimum-order model should include Saturn's rings, asphericity of Mimas, asphericity of Enceladus, Janus, and J_8 along with the 1996 JPL baseline.

Numerical results validate this conclusion. Using the prescribed minimum model, we are able to numerically match the truth model to an accuracy of 1.1 km or better for all the satellites as shown in Fig. 11 (with the satellites labeled from top to bottom in descending order of maximum perturbation). The resulting maximum errors are 1.06 km for Mimas, 0.66 km for Enceladus, 0.19 km for Tethys, 0.31 km for Dione, 0.03 km for Rhea, 0.09 km for Titan, 0.18 km for Hyperion, and 0.07 km for Iapetus. The required changes in the satellite initial conditions are less than 3 m and 0.8 mm/s. Thus, this minimum-order model fulfills the requirements of the study with an unobservable change in the initial state.

Conclusion

Two methods are presented for determining the effects that must be retained in a model to achieve a given accuracy. Using a fixed set of IC's provides a conservative assessment. Our opinion is, however, that the results for adjusted IC's provide a more realistic guide for determining the effects that must be modeled. The IC's themselves are not perfectly known quantities, but are solved for in the orbit determination process. Therefore, allowing minor adjustments in the state seems reasonable. With this approach, adding the effects of Saturn's rings, Janus, J_8, and asphericities of Mimas and Enceladus to the 1996 JPL baseline model ensures 1 km accuracy over four years. The modeling of the rings can be accomplished using either the elliptic function formulation or zonal harmonics.

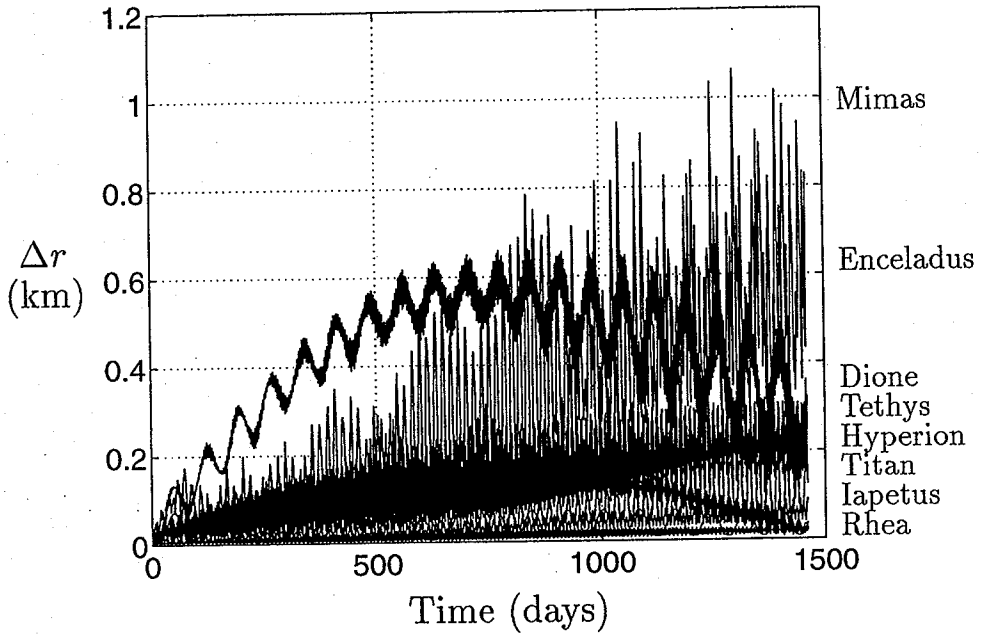

FIG. 11. Comparison Between Minimum-Order Model and Truth Model (Adjusted IC's).

Acknowledgments

We wish to thank Jeremy Jones of the Jet Propulsion Laboratory for his guidance and Robert Jacobson for providing assistance with the simulations. Also, we thank Jeremy Jones, Robert Jacobson and Claude Hildebrand for many valuable discussions.

This work has been supported by the Cassini Project of the Jet Propulsion Laboratory, California Institute of Technology, Contract Number 960620.

References

[1] JONES, J. B., HILDEBRAND, C. E., and JACOBSON, R. A. Private communication, 1996, Jet Propulsion Laboratory, Pasadena, CA.

[2] CHOBOTOV, V. A. *Orbital Mechanics,* American Institute of Aeronautics and Astronautics, Inc., Washington, D.C., 1991.

[3] GAVRILOV, S.V. and ZHARKOV, V. N. "Love Numbers of the Giant Planets," *Icarus,* Vol. 32, 1977, pp. 443–449.

[4] LOVE, A. E. H. *Some Problems of Geodynamics,* Dover Publications, Inc., New York 1967, pp. 49–57.

[5] BURNS, J. A. (editor) *Planetary Satellites,* The University of Arizona Press, Tucson, AZ, 1977, pp. 113–156.

[6] PEALE, S. J., CASSEN, P., and REYNOLDS, R. T. "Tidal Dissipation, Orbital Evolution, and the Nature of Saturn's Inner Satellites," *Icarus,* Vol. 43, 1980, pp. 65–72.

[7] KROGH, F. T., NG, E.W., and SNYDER, W.V. "The Gravitational Field of a Disk," *Celestial Mechanics,* Vol. 26, 1982, pp. 395–405.

[8] SCHEERES, D. J. and VINH, N. X. "Satellite Dynamics about a Planet with a Narrow Ring," *Advances in the Astronautical Sciences: Spaceflight Mechanics,* Vol. 82, Part II, 1993, pp. 747–764.

[9] LASS, H. and BLITZER, L. "The Gravitational Potential Due to Uniform Disks and Rings," *Celestial Mechanics,* Vol. 30, 1983, pp. 225–228.

[10] McCUSKY, S.W. *Introduction of Celestial Mechanics,* Addison-Wesley Publishing Co., Reading, Massachusetts, 1963.

[11] GOLDREICH, P. and PEALE, S. J. "Spin-Orbit Coupling in the Solar System," *The Astronomical Journal,* Vol. 71, No. 6, pp. 425–438.

[12] VINH, N. X. "Sur Les Solutions Périodiques du Mouvement Plan de Libration des Satellites et des Planètes," *Celestial Mechanics,* Vol. 8, pp. 371–403, 1973.

[13] MEASE, K. D., WOOD, L. J., BERGAM, M. J., and WHITE, L. K. "Estimation of Solar Gravitational Harmonics with Starprobe Radiometric Tracking Data," *Journal of the Astronautical Sciences,* Vol. 31, No. 1, pp. 3–22.

[14] WILL, C. F. "The Theoretical Tools of Experimental Gravitation," *Experimental Gravitation,* Bertotti, B., ed., Academic Press, New York, 1974, pp. 1–105.

[15] ZHARKOV, V. N., LEONTJEV, V.V., and KOZENKO, A.V. "Models, Figures, and Gravitational Moments of the Galilean Satellites of Jupiter and Icy Satellites of Saturn," *Icarus,* Vol. 61, 1985, pp. 92–100.

[16] CAMPBELL, J. K. and ANDERSON, J. D. "Gravity Field of the Saturnian System from Pioneer and Voyager Tracking Data," *The Astronomical Journal,* Vol. 97, No. 3, May 1989, pp. 1485–1495.

[17] DANBY, J. M. *Fundamentals of Celestial Mechanics,* The Macmillan Company, New York, 1962.